01 Jan 2023

Measurement of Volumetric Deformation, Strain Localization, and Shear Band Characterization during Triaxial Testing using a Photogrammetry-Based Method

Sara Fayek

Xiong Zhang
Missouri University of Science and Technology, zhangxi@mst.edu

Xiaolong Xia

Qingqing Fu

et. al. For a complete list of authors, see https://scholarsmine.mst.edu/civarc_enveng_facwork/2507

Recommended Citation

S. Fayek et al., "Measurement of Volumetric Deformation, Strain Localization, and Shear Band Characterization during Triaxial Testing using a Photogrammetry-Based Method," *Geotechnical Special Publication*, no. GSP 340, pp. 466 - 476, American Society of Civil Engineers, Jan 2023.
The definitive version is available at https://doi.org/10.1061/9780784484678.047

Measurement of Volumetric Deformation, Strain Localization, and Shear Band Characterization during Triaxial Testing Using a Photogrammetry-Based Method

Sara Fayek, S.M.ASCE[1]; Xiong Zhang, Ph.D., P.E.[2]; Xiaolong Xia[3]; Qingqing Fu[4]; and Jeffrey Cawlfield, Ph.D., P.E.[5]

[1]Ph.D. Candidate, Dept. of Civil, Architectural, and Environmental Engineering, Missouri Univ. of Science and Technology, Rolla, MO. Email: fayeks@umsystem.edu
[2]Professor, Dept. of Civil, Architectural, and Environmental Engineering, Missouri Univ. of Science and Technology, Rolla, MO. Email: zhangxi@umsystem.edu
[3]Graduate Student, Dept. of Civil, Architectural, and Environmental Engineering, Missouri Univ. of Science and Technology, Rolla, MO. Email: xxrkq@umsystem.edu
[4]Graduate Student, Dept. of Civil, Architectural, and Environmental Engineering, Missouri Univ. of Science and Technology, Rolla, MO. Email: qfg2f@umsystem.edu
[5]Professor, Dept. of Geosciences, Geological, and Petroleum Engineering, Missouri Univ. of Science and Technology, Rolla, MO. Email: jdc@umsystem.edu

ABSTRACT

Triaxial testing has been routinely used as a standard laboratory test that allows correct determination of soil characteristics. Previously the volumetric strain of the triaxial specimen was considered to be uniformly distributed along with the specimen during the isotropic and deviatoric loading. Although this assumption might hold true under isotropic loading, the effects of restrained ends and disturbance during the procedures of specimen installation and testing can cause nonuniform strains throughout the whole specimen. This paper investigates the effects of specimen preparation and misalignment on the strain uniformity along with the soil specimen during triaxial testing. A series of consolidated drained tests at several stress paths were conducted on sand specimens. A photogrammetry-based method was applied at different stages of specimen preparation and testing to provide a three-dimensional full-field deformation measurement of the surface of the triaxial soil specimen. One commercial camera was used to capture images for the triaxial specimen, and a developed application for data processing and post-processing was utilized to ensure automatic and fast processing of the developed photogrammetric-based method. The local displacement data provided by the photogrammetry-based method enabled the evaluation of the strain localization and the volumetric strain nonuniformity analysis at different heights along with the specimen. The triaxial test results demonstrated that the soil specimen during triaxial testing has deformed nonuniformly in the axial, radial, and circumferential directions. The plots of the strain localization precisely presented the variation of local strains and the magnitude of deformation after the saturation stage. These results prove the soil specimen volume is not constant during saturation, and unavoidable disturbance had occurred during the specimen preparation steps and saturation. The results proved that the specimen misalignment during triaxial testing leads to scattering in the triaxial test results. Further discussion was presented about the shear band characterization including shear band thickness, formation, and propagation.

Keywords: Triaxial Test, Photogrammetry, 3D full-field displacement, Strain Localization, Shear Band.

INTRODUCTION

Triaxial tests have been intensively used to characterize the behavior of both saturated and unsaturated soils owing to their advantages of providing controlled well-defined boundaries, uniform stresses within the soil, and drainage conditions (Fayek et al. 2022). During triaxial testing, the soil volume and deformation are required to determine the stress-strain relationship of soils. In addition, the accurate measurements of local and total deformation of soil specimens contribute greatly to understanding the characteristics of nonlinearity and anisotropy behavior as well as in the modeling and numerical simulation of soil mechanics (Alshibli et al. 2002; Desrues and Viggiani 2004; Rechenmacher 2006). Quantification of shear band formation, growth, and evolution is a crucial factor in the development of constitutive models of soils (Sachan and Penumadu 2007). However, the triaxial soil specimen is subjected to many sources of disturbance during preparation, installation, and saturation procedures besides the effect of measurement techniques and equipment (Mulilis et al. 1977; Baldi et al. 1988; Santagata 1994; and Scholey et al. 1995). Although previous research provided a useful guideline to understand the effect of disturbance and error measurement on triaxial results, there is not yet a practical and accurate methodology to quantify the effect of sample disturbance during triaxial testing.

In recent years with the improved development of image-based methods in triaxial testing, the measurement of deformation and strain localization has gained increasing focus (Alshibli and Sture 2000). The image-based methods can be classified in terms of their system designs and principles into various categories including Digital image analysis (DIA), digital image correlation (DIC), X-ray computed tomography (CT), and photogrammetric methods (Macari et al. 1997; Gachet et al. 2007; Sachan and Penumadu 2007; Rechenmacher and Medina-Cetina 2007; Bhandari et al. 2012; Zhang et al. 2015). However, many of the previous methods only considered part of the soil specimen and made assumptions about the soil specimen's shape and deformation (Desrues and Viggiani 2004; Lin and Penumadu 2006; Rechenmacher 2006; Bhandari et al. 2012). X-ray CT was able to detect the internal structure of the soil specimen by interpreting the intensity data of the X-ray beam passes through the soil specimen. However, X-ray CT is expensive to be implemented. For the first time, the photogrammetric method was able to determine with cost-effectiveness the full-field deformation of soils during triaxial testing. Photogrammetry is the science of reconstruction of 3D models from 2D images. Zhang et al. (2015) developed a photogrammetry-based method to determine the specimen shape and deformation at any stage of triaxial testing by using only one commercially available camera. Multiple optical ray tracings and a least-square optimization technique were employed for refraction correction at the air-acrylic cell and acrylic cell–water interfaces. Global and local deformation measurements were performed for both saturated and unsaturated soils. However, this method was not able to locate the top and bottom boundaries between the soil sample, the top cap, and the bottom pedestal respectively since the top and bottom boundaries were covered by a membrane during testing. As assumptions were made to determine the soil sample's boundaries, the accuracy of the soil volume measurements is questionable. To overcome this limitation, Fayek et al. (2020) proposed a simple and rigorous photogrammetry-based technique to determine the top and bottom boundaries of the soil specimens mathematically. The principle is based on the fact that the distances from the peripheral coded targets to the surface plane of each pedestal will remain unchanged, regardless of their locations and orientations during the triaxial tests. So, by applying the method proposed by Fayek et al. (2020), the specimen ends and the absolute soil volume were determined with high accuracy without making any assumptions

about the specimen's shape or boundary. More improvement to the method was proposed by Xia et al. (2021) by proposing a table method to make up missing points and allowed automatic and fast processing of measurement targets on the soil specimen's surface. With the implementation of the photogrammetric method of Zhang et al. (2015), the absolute soil volume methodology of Fayek et al. (2020), and the automatic processing presented in Xia et al. (2021), this paper present a new approach that allows an automatic, fast, and accurate method to measure the volumetric deformation, strain localization, and shear band characterization during triaxial testing.

This research allows a full-field deformation of soils during various stages of testing. A series of consolidated drained tests at several stress paths were conducted on sand specimens. A photogrammetry-based method was applied at distinct stages of specimen preparation and testing to provide a three-dimensional (3D) full-field deformation measurement of the surface of the triaxial soil specimen. The photogrammetric method proposed by Zhang et al. (2015) and the improvements made by Fayek et al. (2020) and Xia et al. (2021) were applied with minor modifications. One available commercial camera was used to capture images for the triaxial specimen, and a developed application for data processing and post-processing was utilized to ensure automatic and fast processing of the developed photogrammetric-based method. The local displacement data provided by the photogrammetry-based method enabled the evaluation of the strain localization and the volumetric strain nonuniformity analysis at different heights along with the specimen. The comparison of the strain localization at distinct stages of specimen preparation allowed the clarification of the potential sources of specimen disturbance. The triaxial test results demonstrated that the soil specimen during triaxial testing is subjected to an inevitable disturbance that caused deviation from its initial measured dimensions. The results further discuss the formation of the shear band characterization including shear band thickness, formation, and propagation. In addition, a conclusion on the effects of misalignment and specimen preparation on the strain uniformity along with the soil specimen during triaxial testing is made.

EXPERIMENTAL PROGRAM

Specimen Preparation and Triaxial Test Program

The soil used in triaxial testing is clean Ottawa 20-30 sand that conforms to ASTM designated C778. The triaxial soil specimens of 72 mm in diameter were prepared using the moist tamping method. Initially, the sand is oven-dried and sieved through a 0.5 mm screen. Then, the dried soils are thoroughly mixed with a water content of 2 % water, then compacted in 6 layers. The soil specimen can reach the desired density by adjusting the number of tamps per layer, the force per tamp per layer, and the amount of water added during mixing. The under-compaction method, which simulates a relatively homogeneous soil condition, was used to prevent excessive densification of the lowest layers (Ladd 1978). Each subsequent layer received less percentage of under-compaction, where the tamping energy is gradually augmented from the bottom to the top layer so that uniform density can be obtained throughout the specimen layers. In addition, the top of each compacted layer was scarified before the addition of material for the next layer to ensure good contact with the subsequent soil layer. This process was repeated until a full height of 144 mm was reached for the soil specimen of a relative density of 70%. Then the mold was removed, and the membrane was sealed at the top cap and base pedestal with rubber O-rings. After that, the triaxial chamber was assembled and filled with water.

Initially, the soil specimen was percolated with carbon dioxide gas for 45 minutes to push the air up through the top drainage line. Then, the soil sample was slowly flushed with de-aired water to push most of the carbon dioxide out. Any carbon dioxide that remained in the specimen can be dissolved in the intruding water, and subsequently, fill the voids in the soil specimen. To ensure that the specimen is fully saturated, the back-pressure saturation procedure was applied until the measurement of the B-value (B-pore pressure parameter) reached at least 0.98. Other specimens were prepared with the same water content and similar preparation procedure but tested at different stress path. For this paper, the results are presented for only one specimen. The specimen was isotropically compressed to 200 kPa, then unloaded to 50 kPa, and later reloaded to 300 kPa. The specimen was sheared by advancing the axial piston downward, with a strain rate of 0.5% per hour, under a constant confining pressure of 300 kPa until failure. The volume of water exchange from the sample, the axial load-deformation, and the volume change were recorded.

Photogrammetry-Based Method: Implementation and System Setup

The photogrammetric method proposed by Zhang et al. (2015) besides the improvement made by Fayek et al. (2020) and Xia et al. (2021) were applied in this research with slight modification. The conventional triaxial test apparatus for saturated soils, pressure sensors, digital controllers, and a close-range photogrammetry-based system were used to measure the displacement of soil specimens after each preparatory, compression, and shearing stage (Figure 1). One minor modification was applied to the top cap and bottom pedestal by partially engraving their surface to place porous stones. To prevent the block view caused by the drainage lines in the triaxial chamber, the drainage lines connecting the top pedestals with the triaxial cell base were relocated to be connected with the triaxial cell top.

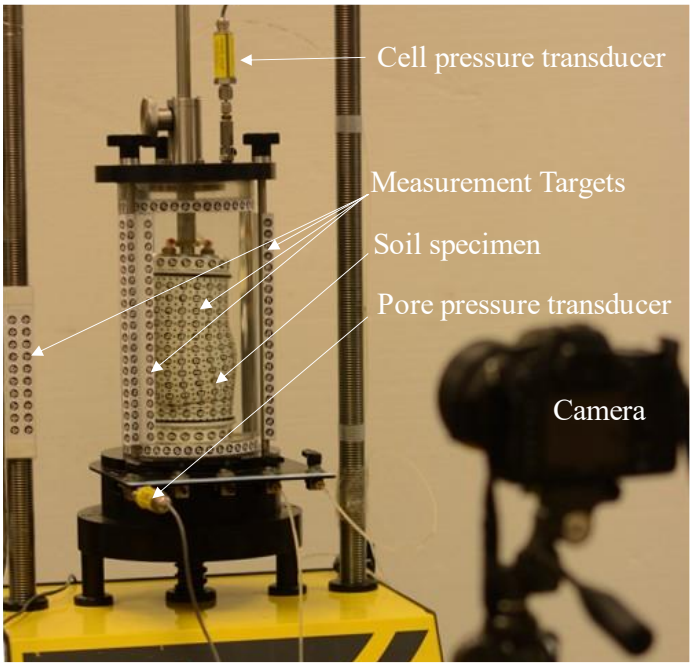

Figure 1. Triaxial testing system presenting a deformed soil specimen during the shearing phase.

The close-range photogrammetry system used during triaxial testing consisted of the following:

(1) A commercially available digital camera (Nikon D7000) with a 50-mm fixed focal length lens (AF-S Nikkor 50mm f/1.4 G) to capture the images. The camera has an image sensor with a resolution of 16.2 million pixels (4928 H: 3264 V). The camera was fully calibrated before initiating the triaxial testing to acquire accurate and reliable 3D metric information from the captured images.
(2) A photogrammetry commercial software for the camera calibration process.
(3) A developed MATLAB program for data post-processing. The top and bottom boundaries between the soil specimen, and the top cap and bottom pedestal, were determined using the developed program. Also, the specimen surface interpolation, volume calculation, displacement, and strain were automatically calculated.
(4) A latex membrane with a total number of 816 measurement targets consisting of 204 black-ringed automatically detected (RAD) coded targets and 612 black dots printed on its surface.

Additional RAD targets were posted on the outside surface of the acrylic chamber, including two circles and three vertical stripes to determine the cell wall deflection and the cell shape and location at different confining pressure during testing. Also, RAD targets were posted on the triaxial cell tie rods and load frame to provide overlapping points between the captured images and enable the establishment of a global coordinate system for the photogrammetry-based analysis. In addition to that, measurement targets were placed on the top surface and periphery of both the top cap and bottom pedestal. Using a digital caliper, several measurements between RAD targets were acquired to define the scale as an input in the MATLAB app. The procedure of the photogrammetry-based method for determining the deformation of the soil specimen during triaxial testing can be summarized in the following steps:

- *Camera calibration*: To achieve a high level of measurement accuracy in the photogrammetric analysis, the camera calibration process is required. Since commercially available cameras often use multiple lenses, slight bending of the light rays either outward or inward is caused. Thus, the camera should be calibrated to get precise and reliable 3D reconstruction of the soil specimen. In this study, the calibration process was performed using a single calibration sheet. The calibration is performed by capturing using the camera around 12 images of the calibrated sheet. By analyzing these images, the intrinsic and extrinsic parameters were calculated.
- *Photographing*: The calibrated camera was used to capture images around the triaxial apparatus at a different stage of triaxial testing. First, images were captured for the top cap and bottom pedestals independently which can be used to back-calculate the specimen's boundaries with the top cap and bottom pedestal. Additional pictures were taken for the assembled model during triaxial testing. More details about the process of back calculating the top and bottom boundaries of the soil specimen are presented in Fayek et al. (2020).
- *Photogrammetric analysis*: The camera calibration parameters were imported in the MATLAB app. Then the camera orientations, location, and the 3D coordinates of the targets were determined by the photogrammetric analysis. During this process, the acrylic cell shape and deformation were acquired for the ray-tracing technique and the least-square optimization technique. More details about this procedure can be found in Zhang et al. (2015).

- *Post-Processing*: After acquiring the 3D coordinates of the targets on the surface of the soil specimen, the top and bottom boundaries between the soil specimen, the top cap, and the bottom pedestal were back-calculated (Fayek et al. 2022b). The displacement and strain localization calculations were determined using the method described by Lin and Penumadu (2006) as presented in the following section.

STRAIN LOCALIZATION: INTERPOLATION AND CALCULATIONS

The photogrammetry-based method is used to evaluate the deformation of the soil specimen during triaxial testing. The 3D coordinates of the 816 discrete measurement points on the soil surface were determined at desired time intervals (Figure 2.a). Then, the 3D coordinates at two different time intervals were compared, for example comparing the 3D coordinates after saturation to those at the initial condition in the air. The displacement of each measurement target during each time interval was calculated. The strain localization calculations were adopted from Lin and Penumadu (2006). A small 3D block was separated from the specimen, as shown in Figure 2.b, with four targets on the outside surface whose 3D coordinates are measured using the photogrammetric method. The depth of the block is considered to be around 10 mm. This block is further divided into five irregular tetrahedrons where each point of the tetrahedron has three displacement components including vertical displacement, u_1; radial displacement, u_2; and circumferential displacement, u_3.

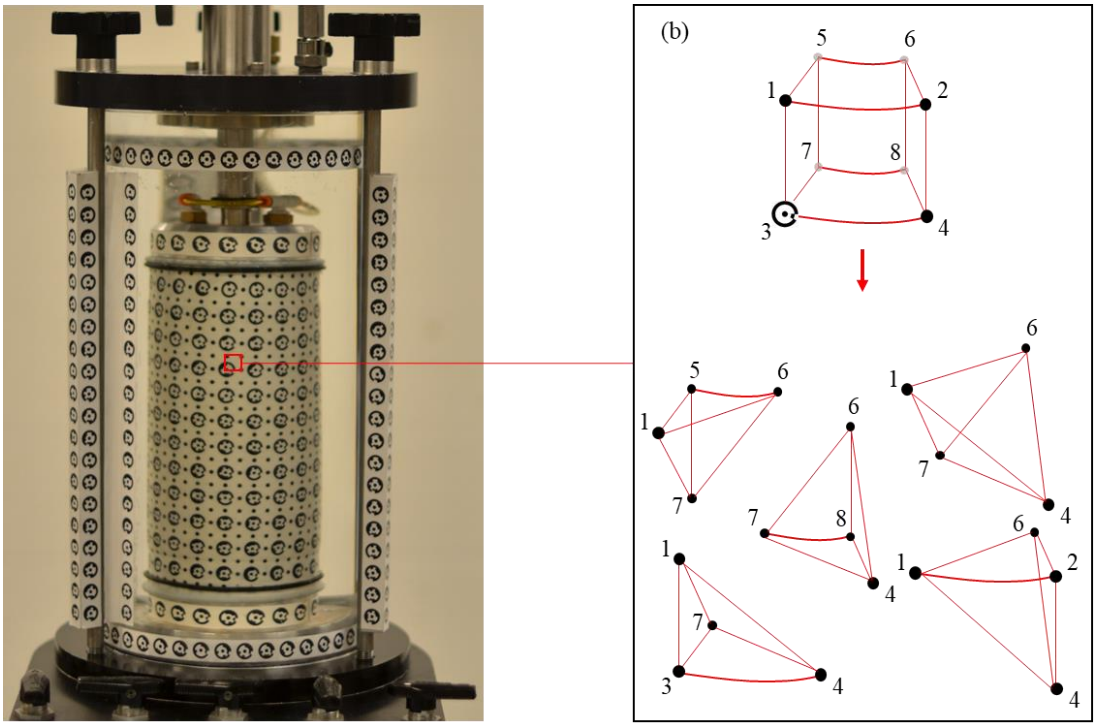

Figure 2. (a) Targets printed on the membrane surface; (b) The 3D cube and its divided five four-surface elements (Modified from Lin and Penumadu (2006)).

The displacement of any point within the element was assumed to be a linear function of the coordinates z, r, and θ as per Equation 1 (Lin and Penumadu 2006) as follows:

$$u_m = a_{m0} + a_{m1}z + a_{m2}r + a_{m3}\theta \quad (1)$$

where a_{mn} (m=1 to 3, n=0 to 3) are constant to be determined.

Using Lin and Penumadu (2006) suggested procedure, the local strain components can be solved using Equation (2). It is worth noting that Equation 2 was corrected using finite element theory as follows:

$$\begin{Bmatrix} \varepsilon_z \\ \varepsilon_r \\ \varepsilon_\theta \\ \varepsilon_{r\theta} \\ \varepsilon_{rz} \\ \varepsilon_{\theta z} \end{Bmatrix} = \begin{Bmatrix} \dfrac{\partial u_1}{\partial z} \\ \dfrac{\partial u_2}{\partial r} \\ \dfrac{u_2}{r} \\ \dfrac{1}{2}\left(\dfrac{\partial u_3}{\partial r} + \dfrac{\partial u_3}{r\partial \theta} - \dfrac{u_3}{r} \right) \\ \dfrac{1}{2}\left(\dfrac{\partial u_1}{\partial r} + \dfrac{\partial u_2}{\partial z} \right) \\ \dfrac{1}{2}\left(\dfrac{\partial u_2}{r\partial \theta} + \dfrac{\partial u_3}{\partial z} \right) \end{Bmatrix} \quad (2)$$

The displacement components of points 5, 6, 7, and 8 can be calculated considering a linear relationship with points 1, 2, 3, and 4. The vertical, radial, and circumferential displacements of points 5, 6, 7, and 8 are presented in Equations 3, 4, and 5 respectively as follows:

$$u_{15} = u_{11};\ u_{16} = u_{12};\ u_{17} = u_{13};\ u_{18} = u_{14} \quad (3)$$

$$u_{25} = u_{21} * \frac{r_5}{r_1};\ u_{26} = u_{22} * \frac{r_6}{r_2};\ u_{27} = u_{23} * \frac{r_7}{r_3};\ u_{28} = u_{24} * \frac{r_8}{r_4} \quad (4)$$

$$u_{35} = u_{31} * \frac{r_5}{r_1};\ u_{36} = u_{32} * \frac{r_6}{r_2};\ u_{37} = u_{33} * \frac{r_7}{r_3};\ u_{38} = u_{34} * \frac{r_8}{r_4} \quad (5)$$

RESULTS

Using the 3D coordinates obtained from the photogrammetry-based method and the formulation presented in the previous section, the displacement and strain components were calculated. To facilitate the visualization of the uniformity of deformation and the strain localization of the soil specimen, contour plots are used to illustrate the 3D surface displacement and strain localization. The points that share the same value of displacement or strain are connected by contours with different colors that represent the value corresponding to the displacement or strain. To generate a full-field continuous deformation of the specimen, a numerical interpolation technique was used between the discrete measurement points. Figure 3

shows the 3D full-field displacement and strain localization of the soil specimen after saturation. The intensity of the color on the contour plots represents the magnitude of the corresponding displacement or strain. Following the convention used in geotechnical engineering, a negative sign for displacement and strain represents extension, and a positive sign represents compression. It can be noticed that the soil specimen has deformed nonuniformly after saturation with a maximum of 2 mm, 1 mm, and 0.04º in the axial, radial, and circumferential directions, respectively. Strains values vary between 0 and 0.08, -0.04 and 0.04, and -0.04 and 0.04 in the axial, radial, and circumferential directions, respectively. The specimen response is non-uniform in the axial, radial, and circumferential strain, and they are positive in the left half of the specimen. Negative displacement and strain were noticed on the right side of the soil specimen. As the specimen was assumed to have negligible disturbance during the specimen preparation and saturation stages, theoretically, no strain localization was expected. However, the plots of the strain localization accurately present the variation of local strains and the magnitude of deformation after the saturation stage. These results prove the soil specimen volume is not constant during saturation and unavoidable disturbance had occurred during the specimen preparation steps and saturation.

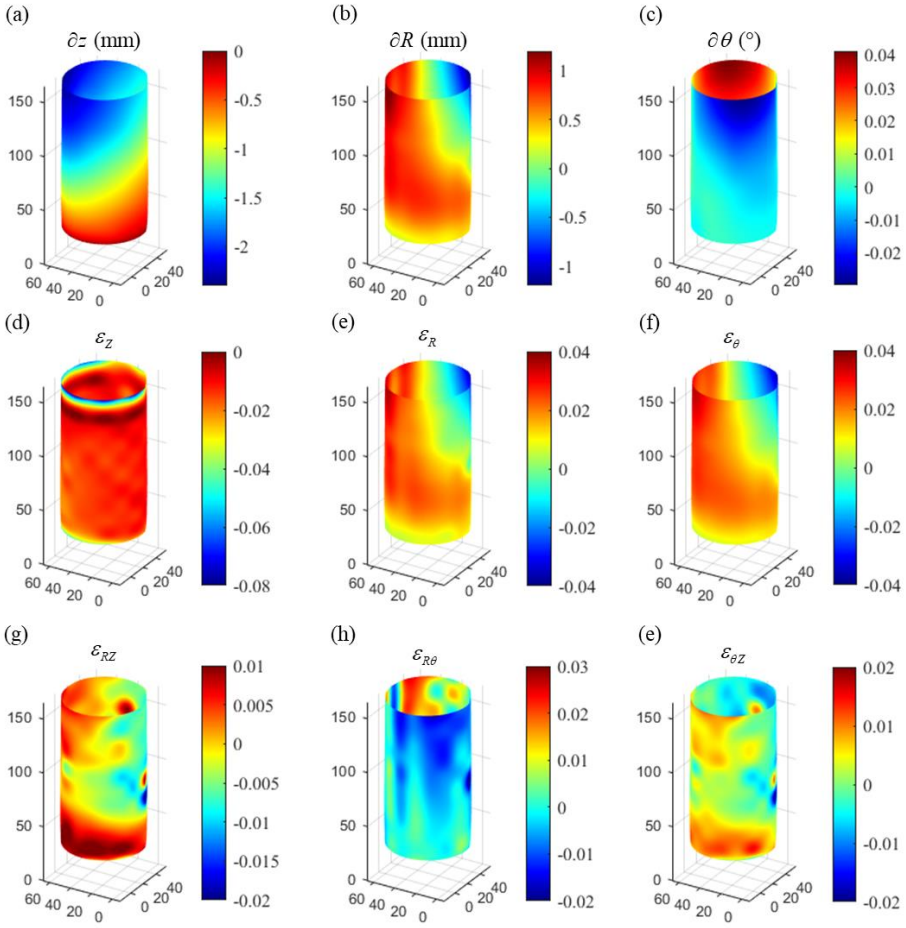

Figure 3. 3D full-field displacement and strain localization: (a) axial displacement, (b) radial displacement, (c) circumferential displacement, (d) axial strain, (e) radial strain, (f) circumferential strain, (g) ε_{RZ} (h) $\varepsilon_{R\theta}$ (e) $\varepsilon_{\theta Z}$.

Similarly, the circumferential strain at the end of the shearing stage was calculated and presented as shown in Figure 4. This result is the best presentation of the trend of development of the shear band. The angle and thickness of the shear band were derived from the contours on the soil specimen. The shear band with clear inclination starts developing at 3% global vertical strain and becomes more significant with the increase of global vertical strain. The inclination and the thickness of the shear band, denoted by θ and t respectively, were determined by the dense color of the contour lines. In addition, it can be noticed from Figure 4 that the top edge of the soil specimen is not horizontal at the end of the shearing stage. The tilting of the top cap or soil specimen can be attributed to many factors as described by Fayek et al. (2022c). The excess deformation or formation of the shear band can be correlated to the misalignment of the soil specimen. This result is also related to the findings of Fayek et al. (2022c) where the misaligned specimen demonstrated higher deformation compared to the idealized aligned specimen case. This proves that the specimen misalignment during triaxial testing leads to scattering in the triaxial test results. Specimen misalignment alters the strain distribution uniformity in the triaxial specimen and resulted in higher strain values. This influence becomes larger and larger with increasing strains and these nonuniformities can significantly influence the estimation of the soil shear strength properties. Discussions regarding vertical displacement, tilting, and eccentricity can be found in (Fayek et al. 2022a; Fayek et al. 2022c).

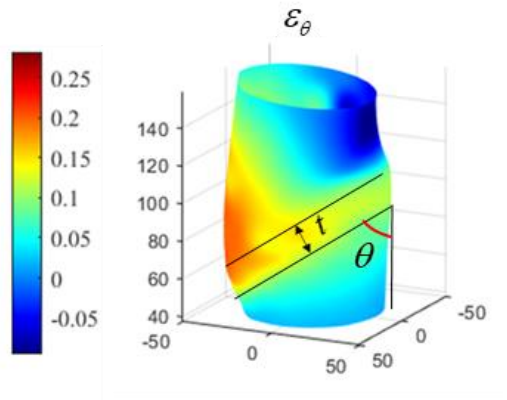

Figure 4. 3D full-field circumferential strain showing the shear band inclination and propagation.

CONCLUSION

A noncontact photogrammetry-based method was used to reconstruct an accurate 3D full-field model of the soil specimen at any stage of triaxial testing. Further analysis was performed to determine the specimen's ends and the absolute soil volume. In addition, the strain localization was calculated using the finite element theory. Based on the displacement and strain localization results, the soil was noticed to be deformed non-uniformly after the saturation process. This confirms that the saturation process can disturb the soil specimen and that the volume of soil during the preparatory and saturation stage is not constant. During deviatoric loading, the soil has further deformed, and a shear band was formed. The calculation of the shear band inclination can be easily derived from the color of contour lines. Based on the measurement results on the triaxial soil specimen, it could be concluded that the photogrammetry-based method proposed is

a powerful tool for an in-depth understanding of soil behavior during triaxial testing. More details on the comprehensive evaluation of important aspects of triaxial testing using the photogrammetry-based method can be found in Fayek et al. (2023).

REFERENCES

Alshibli, K., and Sture, S. (2000). "Shear band formation in plane strainexperiments of sands." *J. Geotech. Geoenviron. Eng.*,126(6), 495–503.

Alshibli, K. A., Sture, S., Costes, N. C., Frank, M. L., Lankton, M. R., Batiste, S. N., and Swanson, R. A. (2000). "Assessment of localized deformations insand using x-ray computed tomography." *Geotechn. Test. J.*, 23(3), 274–299.

Baldi, G., Hight, D. W., and Thomas, G. E. (1988). *A reevaluation of conventional triaxial test methods*.ASTM STP977, ASTM, West Conshohoeken, Pa., 219–263.

Bhandari, A. R., Powrie, W., and Harkness, R. M. (2012). "A digital image-based deformation measurement system for triaxial tests." *Geotechn. Test. J.*, 35(2), 209-226.

Desrues, J., and Viggiani, G. (2004). "Strain localization in sand: an overview of the experimental results obtained in Grenoble using stereophotogrammetry." *Int. J. Numer. Anal. Methods Geomech.*, 28(4), 279-321.

Fayek, S., Xia, X., Li, L., and Zhang, X. (2020). "Photogrammetry-based method to determine the absolute volume of soil specimen during triaxial testing." *Transportation Research Record*, 2674(8), Transportation Research Board, Washington, D.C., 206-218.

Fayek, S., Xia, X., and Zhang, X. (2022a). "Consideration of One Camera Photogrammetry-Based Method to Reevaluate Some Aspects of Conventional Triaxial Testing." In *Geo-Congress 2022*, 141-151.

Fayek, S., Zhang, X., Galinmoghadam, J., and Cawlfield, J. (2022b). "Point Density for Soil Specimen Volume Measurements in Image-based Methods During Triaxial Testing." *Acta Geotech.* (Tentatively accepted).

Fayek, S., Zhang, X., Galinmoghadam, J., and Xia, X. (2022c). "Evaluating the Effects of Specimen Misalignment during Triaxial Testing Using a Photogrammetry-Based Method," *Geotechn. Test. J.*, (Under Review).

Fayek, S., Zhang, X., and Xia, P. (2023). "Comprehensive Evaluation of Important Aspects of Triaxial Testing Using a Photogrammetry-based Method," *Transportation Research Record*, (Tentatively accepted).

Gachet, P., Geiser, F., Laloui, L., and Vulliet, L. (2007). "Automated digital image processing for volume change measurement in triaxial cells." *Geotechn. Test. J.*, 30(2), 98-103.

Ladd, R. S. (1978). "Preparing test specimens using undercompaction." *Geotechn. Test. J.*, 1(1), 16-23.

Lin, H., and Penumadu, D. (2006). "Strain localization in combined axial-torsional testing on kaolin clay." *J. Eng. Mech.*, 132(5), 555-564.

Macari, E. J., Parker, J. K., and Costes, N. C. (1997). "Measurement of volume changes in triaxial tests using digital imaging techniques." *Geotechn. Test. J.*, 20(1), 103-109.

Mulilis, J. P., Seed, H. B., Chan, C. K., Mitchell, J. K., and Arulanandan, K. (1977). "Effects of sample preparation on sand liquefaction." *J. Geotech. Eng. Division*, 103(2), 91-108.

Rechenmacher, A. L. (2006). "Grain-scale processes governing shear band initiation and evolution in sands." *J. Mech. Phys. Solids*, 54(1), 22-45.

Rechenmacher, A. L., and Medina-Cetina, Z. (2007). "Calibration of soil constitutive models with spatially varying parameters." *J. Geotech. Geoenviron Eng.*, 133(12), 1567-1576.
Sachan, A., and Penumadu, D. (2007). "Strain localization in solid cylindrical clay specimens using digital image analysis (DIA) technique." *Soils Found.*, 47(1), 67-78.
Santagata, M. C. (1994). *Simulation of sampling disturbance in soft clays using triaxial element tests* (Doctoral dissertation, Massachusetts Institute of Technology).
Scholey, G. K., Frost, J. D., Presti, D. L., and Jamiolkowski, M. (1995). "A review of instrumentation for measuring small strains during triaxial testing of soil specimens." *Geotechn. Test. J.*, 18(2), 137-156.
Xia, X., Zhang, X., Fayek, S., and Yin, Z. (2021). "A table method for coded target decoding with application to 3-D reconstruction of soil specimens during triaxial testing." *Acta Geotech.*, 16(12), 3779-3791.
Zhang, X., Li, L., Chen, G., and Lytton, R. (2015). "A photogrammetry-based method to measure total and local volume changes of unsaturated soils during triaxial testing." *Acta Geotech.*, 10(1), 55-82.